HHS Public Access

Author manuscript

Acta Physiol (Oxf). Author manuscript; available in PMC 2022 June 01.

Published in final edited form as:

Acta Physiol (Oxf). 2021 June ; 232(2): e13657. doi:10.1111/apha.13657.

Macrophage activation in stellate ganglia contributes to lung injury-induced arrhythmogenesis in male rats

Juan Hong[#1], **Ryan J. Adam**[#1,2], **Lie Gao**[2], **Taija Hahka**[1], **Zhiqiu Xia**[1], **Dong Wang**[3], **Thomas A. Nicholas**[1], **Irving H. Zucker**[2], **Steven J. Lisco**[1], **Han-Jun Wang**[1,2]

[1]Department of Anesthesiology, University of Nebraska Medical Center, Omaha, NE, USA

[2]Department of Cellular and Integrative Physiology, University of Nebraska Medical Center, Omaha, NE, USA

[3]Department of Pharmaceutical Sciences, University of Nebraska Medical Center, Omaha, NE, USA

[#] These authors contributed equally to this work.

Abstract

Aim: Patients suffering from acute lung injury (ALI) are at high risk of developing cardiac arrhythmias. We hypothesized that stellate ganglia (SG) neural inflammation contributes to ALI-induced arrhythmia.

Methods: We created an ALI rat model using a single tracheal instillation of bleomycin (2.5 mg/kg), with saline as a sham control. We recorded ECGs by implanted radiotelemetry in male bleomycin and sham rats treated with and without oral minocycline (20 mg/kg/d), an anti-inflammatory drug that inhibits microglia/macrophage activation. The SG neuronal excitability was assessed by electrophysiology experiments.

Results: ECG data showed that bleomycin-exposed rats exhibited significantly more spontaneous premature ventricular contractions (PVCs) from 1- to 3-week post-induction compared with sham rats, which was mitigated by chronic oral administration of minocycline. The bleomycin-exposed rats displayed a robust increase in both the number of Iba1-positive macrophages and protein expression of interferon regulatory factor 8 in the SG starting as early at 1-week post-exposure and lasted for at least 4 weeks, which was largely attenuated by minocycline. Heart rate variability analysis indicated autonomic imbalance during the first 2-week

Correspondence: Han-Jun Wang, Department of Anesthesiology, University of Nebraska Medical Center, Omaha, NE 68198, USA. hanjunwang@unmc.edu.

AUTHOR CONTRIBUTIONS

JH and RJA generated and analysed data and wrote the original draft manuscript; LG generated and analysed data; TH, ZQX and TAN participated in data curation; DW conceptually designed the study; IHZ, SJL and HJW conceptually designed the study, reviewed, edited and finalized the manuscript.

CONFLICT OF INTEREST

The authors declare no competing interests.

DATA AVAILABILITY STATEMENT

The data that support the findings of this study are available from the corresponding author upon reasonable request.

SUPPORTING INFORMATION

Additional Supporting Information may be found online in the Supporting Information section.

post-bleomycin, which was significantly attenuated by minocycline. Electrical stimulation of the decentralized SG triggered more PVCs in bleomycin-exposed rats than sham and bleomycin + minocycline rats. Patch-clamp data demonstrated enhanced SG neuronal excitability in the bleomycin-exposed rats, which was attenuated by minocycline. Co-culture of lipopolysaccharide (LPS)-pretreated macrophages with normal SG neurons enhanced SG neuronal excitability.

Conclusion: Macrophage activation in the SG contributes to arrhythmogenesis in bleomycin-induced ALI in male rats.

Keywords

acute lung injury; arrhythmogenesis; autonomic dysfunction; cardiopulmonary afferents; neural inflammation; sympatho-excitation

1 | INTRODUCTION

Pulmonary and cardiovascular diseases are leading causes of morbidity and mortality worldwide. Lung injury often causes cardiac pathology and vice versa. For example, patients with chronic obstructive pulmonary disease (COPD) or lung resection often exhibit cardiac arrhythmias including atrial fibrillation and ventricular arrhythmias.[1–4] An understanding of primary lung injury-evoked cardiac arrhythmias is central to the management of these patients. Clinical and preclinical studies, in the field of critical care medicine, have been heavily focused on the mechanical interaction between these two organs such as positive pressure ventilation, its effects on right and left ventricular pre- and afterload, and ventricular interdependence.[5–8] However, little attention has been given to potential neural excitatory mechanisms underlying primary lung injury-evoked cardiac arrhythmias.

The autonomic nervous system is known to play a role in the genesis and maintenance of ventricular arrhythmias.[9,10] The majority of sympathetic postganglionic axons innervating the heart originate from stellate ganglia (SG) cell bodies. Bilateral SG resection has an anti-arrhythmic effects in patients with refractory ventricular tachycardia, suggesting that the SG plays an important role in regulating ventricular arrhythmias.[11–13] Whether the SG is involved in primary lung injury-induced arrhythmias remains unknown. If such pathology can be demonstrated, it would be critical to identify the molecular mechanisms underlying SG neuronal dysfunction in lung injury. Previous studies have reported increased immune cell infiltration in the SG of patients with severe ventricular arrhythmias.[14] However, whether neuroinflammation, especially macrophage activation, occurs in the SG after lung injury has not been investigated. Furthermore, a cause-effect relationship between macrophage activation and the enhanced SG neuronal excitability following lung injury remains to be established. In this study, we hypothesized that lung injury causes macrophage activation in SG, resulting in enhanced SG neuronal excitability which, in turn, increases the incidence of cardiac arrhythmias.

2 | RESULTS

2.1 | Bleomycin-induced lung and heart histology

Rats receiving bleomycin installation exhibited significant lung lesions at necropsy (Figure 1A). Masson-Trichrome staining (Figure 1B) showed that bleomycin-induced extensive collagen deposition in the lungs was indicated by extensive areas of fibrosis. The lungs of sham rats had no lesions. We did not observe any significant cardiac damage or cardiac fibrosis or T-cell infiltration in sham or bleomycin rats (Figure 1C,D).

2.2 | SG macrophage activation post-lung injury

Our data demonstrate that the number of Iba1-positive cells were markedly increased starting at 1-week post-bleomycin instillation and lasted through 4 weeks ($P < .001$; Figure 2A,B), indicating significant macrophage infiltration into the SG post-lung injury. Furthermore, quantitative measurement of interferon regulatory factor 8 (IRF8) (a critical regulatory factor for pro-inflammatory macrophage/microglia activation)[15,16] was also increased 1-week and 4-week post-lung injury (wk1: $P = .001$; wk4: $P < .001$; Figure 2C), suggesting that these infiltrated SG macrophages are primarily pro-inflammatory. Taken together, these data suggest that macrophages were chronically activated in the SG following bleomycin-induced lung injury. Finally, chronic administration of a macrophage inhibitor, minocycline, initiated 3 days prior to bleomycin instillation and given for 4-week post-bleomycin, reduced bleomycin-induced elevation of IRF8 protein expression by 70% in 4-week post-bleomycin rats ($P < .001$ vs bleomycin; Figure 2D), suggesting a long-lasting suppressive efficiency of minocycline on macrophage activation in the SG post-lung injury.

2.3 | Bleomycin-induced arrhythmia was attenuated by minocycline

Compared with sham rats, bleomycin-exposed rat exhibited a markedly increased PVC (up to 400 and 200 per 24 hours at 1-week and 2-week post-bleomycin exposure, respectively; $P < .001$; Figure 3A–C). The number of PVCs in bleomycin-exposed rats continued to increase, albeit modestly, at 3-week post-bleomycin instillation ($P = .049$), and returned to basal levels by Week 4 ($P = .397$). Importantly, chronic administration of minocycline reduced the PVC events to lower levels at 1-, 2- and 3-week post-bleomycin (wk1: $P < .01$, wk2: $P = .001$, wk3: $P = .015$ vs bleomycin rats). No difference was noted in the number of PVCs occurring during the night and day time periods corresponding to the 12-hour light cycle (Figure 3D). We observed no statistically significant differences of atrioventricular (AV) blocks between groups at any time point (Figure S3). We did not observe atrial flutter, atrial fibrillation, atrial tachycardia or ventricular fibrillation in bleomycin rats. We observed a single episode of non-sustained ventricular tachycardia in one bleomycin rat that did not receive minocycline treatment, 1 week following lung injury. Taken together, these data suggest that bleomycin-induced acute lung injury increases the incidence of cardiac arrhythmias, and this effect is largely mitigated by chronic administration of minocycline. It should be mentioned that despite increased PVCs in bleomycin rats, we did not observe any significant change in ECG parameters including HR, PR interval, *P* duration, QRS duration, QT interval or QTc. Minocycline treatment did not result in a significant reduction in PR interval ($P > .05$; Figure S4).

2.4 | Autonomic dysfunction occurs after acute lung injury and is partially prevented by pretreatment with minocycline

As shown in Figure 4, the standard deviation of RR interval (SDRR) was significantly reduced at 2-week post-bleomycin ($P = .015$), but there was no significant reduction at 3 or 4 weeks (wk3: $P = .079$; wk4: $P = .097$). The low frequency to high frequency (LF/HF) ratio was significantly increased in both 1-week and 2-week bleomycin rats (wk1: $P = .030$; wk2: $P = .032$), indicating a pathological shift from cardiac vagal to sympathetic tone after acute lung injury. Moreover, the abnormal SDRR and LF/HF ratio in bleomycin rats were largely prevented by minocycline (SDRR: wk1: $P = .696$, wk2: $P = .022$; LF/HF ratio: wk1: $P = .467$, wk2: $P = .079$; vs bleomycin rats). These results indicate that autonomic dysfunction occurs after acute lung injury and is significantly mitigated by treatment with minocycline.

2.5 | Electrical stimulation of the decentralized SG triggers PVCs in bleomycin rats, which was reduced by chronic minocycline administration

Although the number of spontaneous PVCs was gradually reduced to normal levels in 4-week post-bleomycin, macrophage activation in the SG still existed (Figure 2). Therefore, we suspected that SG neuronal excitability would remain in a high level at this period. To test this hypothesis, we applied direct electrical stimulation to the decentralized right SG at 4-week post-bleomycin to evaluate the generation of PVCs. As shown in Figure 5, electrical stimulation of the decentralized SG in sham rats caused a frequency-dependent increase in HR without any PVC events, whereas the same stimulation triggered a significant increase in PVCs in the 4-week bleomycin rats ($P < .001$ vs sham at 7-Hz stimuli), indicating increased SG excitability in chronic lung injury. These electrical stimulation-induced PVCs were largely attenuated by chronic minocycline treatment ($P < .001$ vs bleomycin rats at 7-Hz stimuli). Because our decentralized SG preparation bypassed both afferent and central pathways, these data suggest a local protective effect of minocycline on the SG.

2.6 | Macrophage activation contributes to increased SG neuronal excitability post-lung injury

Although our decentralized SG stimulation experiments (Figure 5) provided indirect evidence of increased SG neuronal excitability in bleomycin rats, we performed additional experiments to further confirm this observation by direct recordings of SG neuronal activity via patch clamp. We used the current-clamp technique to record the action potential (AP) of DiI-labelled cardiac SG neurons (Figure 6A) in sham and bleomycin rats. As shown in Figure 6, cardiac SG neurons in bleomycin rats exhibited slightly increased resting membrane potential (RMP: $P = .023$ vs sham) and moderately decreased current threshold-inducing APs ($P < .001$ vs sham) in response to a ramp current-stimulation protocol than in sham rats. Furthermore, compared with sham rats, there was also a significant increase in the number of APs in response to a step current-stimulation protocol in cardiac SG neurons in bleomycin rats ($P < .001$). These data provide direct evidence of increased SG neuronal excitability in bleomycin rats. Importantly, we found that chronic minocycline administration largely prevented the abnormalities in AP generation in cardiac SG neurons in bleomycin rats (RMP: $P = .013$; threshold of AP and number of APs: $P < .001$ vs bleomycin rats). There was no significant difference in membrane capacitance of SG

neurons among all three groups (sham, 33.4 ± 3.0 pF; bleomycin, 25.0 ± 3.1 pF; bleomycin + minocycline, 32.4 ± 3.5 pF).

To establish a direct cause-effect relationship between macrophage activation and increased SG neuronal excitability, we co-cultured LPS-pretreated RAW264.7 macrophages (ie pro-inflammatory M1 macrophages) overnight with acutely dissociated adult cardiac SG neurons. As shown in Figure 7, overnight exposure of pro-inflammatory M1 macrophages onto normal cardiac SG neurons significantly lowered AP threshold ($P < .001$) and increased the number of APs (0.01 nA: $P = .044$, 0.02–0.06 nA: $P < .001$) in response to the electrical current injection, indicating that M1 macrophages can sensitize SG neurons. There was no significant difference in membrane capacitance of SG neurons between the two groups (control, 36.3 ± 3.0 pF; LPS, 33.6 ± 3.6 pF). There was no spontaneous AP under resting conditions (ie no current stimulation) when SG neurons were exposed with M1 macrophages. Therefore, our data suggest that exposure of M1 macrophages to normal SG neurons only sensitizes SG neurons but does not intrinsically induce an AP.

3 | DISCUSSION

Lung diseases are often associated with cardiovascular complications.[17] The presence of ventricular arrhythmias in patients with acute or chronic lung injury is reported to be associated with increased mortality, particularly during hospitalization.[18,19] In the current study, we chose a bleomycin-induced lung injury model[20] to study the mechanisms underlying acute lung injury-induced cardiac arrhythmias. In cancer patients, cardiac arrhythmias and ischemic events were detected in combination chemotherapy with cisplatin, etoposide and bleomycin.[21,22] Our data suggest that intra-tracheal delivery of bleomycin is sufficient to recapitulate this cardiac arrhythmogenic phenomenon in rats. Most of the arrhythmias encountered in our study were PVCs, suggesting a ventricular origin in bleomycin rats. PVCs are considered a risk factor for sudden cardiac death.[23] Interestingly, despite increased PVCs, other ECG parameters including PR interval, QRS interval, P duration and QT interval were not significantly different between sham and bleomycin-treated rats. This observation raises the possibility that lung injury-induced cardiac arrhythmias are more likely because of neurogenic mechanisms than direct damage to cardiomyocytes. This hypothesis is supported by our histological examination, demonstrating little evidence of cardiomyocyte damage or cardiac fibrosis in bleomycin rats. Enhanced SG excitability further supports this notion.

Abnormalities in cardiac sympathetic control of the heart are linked to life-threatening arrhythmias and sudden cardiac death.[24–26] Thoracic sympathectomy, removing either one or both SG, has demonstrated benefit as anti-arrhythmic therapy.[12,27–32] This procedure is considered to be widely successful in high-risk patients with long QT syndrome, with a range of arrhythmias and structural heart disease.[12,27,28,31,32] However, a major limitation of this procedure is that it removes normal sympathetic control to the heart. Clearly, an approach that restores SG health rather than outright SG removal would be preferential; however, achievement of this goal requires insight into the mechanisms underlying the molecular and functional abnormalities in the SG in these diseases. The current study demonstrates a novel role for macrophage activation in the SG in mediating cardiac

arrhythmias post-lung injury and suggests a new pharmaceutical therapeutic target for treating cardiac arrhythmias following lung injury. Here, we found that the number of Iba1-positive macrophages was significantly elevated in the SG from 1- to 4-week post-bleomycin. IRF8 protein, which promotes inflammatory macrophage M1 polarization,[33] started to increase at 1-week post-lung injury and continuously increased through 4-week post-bleomycin. Importantly, following chronic administration of minocycline, a wide-spectrum microglia/macrophage inhibitor, the increased number of spontaneous PVCs at 1- to 3-week post-lung injury was largely prevented. At the same time, we confirmed that chronic minocycline administration suppressed IRF8 protein expression in the SG post-bleomycin, suggesting that minocycline prevented macrophage activation in the SG post-bleomycin. These data strongly suggest that macrophage activation in the SG plays an essential role in lung injury-induced cardiac arrhythmias. Because minocycline was systemically administrated, we cannot rule out the possibility that minocycline reduced cardiac arrhythmic events by suppressing microglia/macrophage activation in the central nervous system. Therefore, we performed direct stimulation of the decentralized SG which confirmed a local (SG) anti-arrhythmic effect of minocycline in bleomycin-treated rats. These data show that chronic minocycline administration blocked the increased PVCs induced by the electrical stimulation of the decentralized SG, confirming that macrophage activation in the SG at least, in part, contributes to cardiac arrhythmogenesis post-lung injury.

Additional direct cause-effect relationships between macrophages activation and altered cardiac SG neuronal excitability at the cellular level was provided by cell co-culture studies. Our data show that exposure of pro-inflammatory M1 macrophages onto normal cardiac SG neurons significantly increased normal SG neuronal excitability. Furthermore, we directly compared cardiac SG neuronal excitability between sham and 4-week bleomycin rats. Patch-clamp data confirmed that there was increased cardiac SG neuronal excitability in the bleomycin rats compared with sham rats, which was largely prevented by chronic minocycline administration. These data established a direct contribution of macrophage activation to the enhanced SG neuronal excitability post-lung injury.

The time window for bleomycin-induced spontaneous PVCs did not completely match with the window for SG macrophage activation. Although bleomycin strikingly increased the number of spontaneous PVCs at 1- to 2-week post-bleomycin, these spontaneous PVCs gradually disappeared at later time points. However, macrophage activation in the SG remained through the entire 4-week time course. This mismatch indicates that macrophage activation in the SG per se is not sufficient to produce spontaneous PVCs. Nevertheless, direct electrical stimulation of the decentralized SG in the presence of activated macrophages triggered PVCs in the latter stages (4-week post-instillation) of lung injury. Therefore, it is reasonable to speculate that macrophage activation in the SG sensitizes SG neurons rather than directly activates them to trigger arrhythmias. This concept was also supported by our macrophage/SG neuron co-culture data. The ability to evoke spontaneous PVCs at the early stage of lung injury may suggest the presence of additional neural sympatho-excitatory stimuli to cause SG neuronal firing as well as cardiac arrhythmias. Our heart rate variability (HRV) data analysis including SDRR and LF/HF ratio, both of which have been widely used as an index of cardiac sympatho-vagal balance,[29] provides additional

evidence suggesting enhanced sympatho-excitation in the early stage of lung injury. While our study focused more upon the sympathetic nervous system than the parasympathetic nervous system, it is likely that lung injury with bleomycin affects both. Stimulation of the parasympathetic system could have been a causal factor behind the episodes of AV block arrhythmias we observed, although additional investigation would be required to identify a precise mechanism.

Considering that acute lung injury is associated with moderate to severe pulmonary inflammation and potential systemic hypoxia, we speculated that there might be at least two potential neural reflexes involved in the acute lung injury-driving sympatho-excitatory events: the carotid body (CB) chemoreflex and the pulmonary spinal afferent reflex (PSAR). The CB chemoreflex plays a critical role in oxygen homeostasis for the body. A previous study by Jacono et al reported that afferent sensory input from the CB contributes to a selective enhancement of hypoxic ventilatory drive in early lung injury in the absence of pulmonary fibrosis and arterial hypoxemia.[34] Therefore, it is not surprising that the chemoreflex is activated and drives the increased sympathetic outflow in the bleomycin rats. Furthermore, Cao et al demonstrated that a single intra-tracheal delivery of bleomycin can produce a significant reduction in PO_2 at the first week of lung injury but by day 30 has largely recovered,[35] suggesting that hypoxia occurs in the early phase rather than late stage of bleomycin-induced lung injury. Therefore, it is very likely that a chemoreflex activation occurs during the first and second weeks after bleomycin and contributes to sympatho-excitation after lung injury. On the other hand, we believe that the PSAR plays a critical role in driving increased central sympathetic flow to the SG during acute lung injury. Our recent studies demonstrated that stimulation of the PSAR by chemical activation of pulmonary sympathetic spinal afferents acutely increases blood pressure, heart rate and renal sympathetic nerve activity in the vagotomized rats,[36] indicating a pro-sympathetic role for these afferents. Although we did not perform a comprehensive analysis of lung pathology in this study, the time course of bleomycin-induced lung inflammation is already very well established. For example, the study by Chaudhary et al used a similar dose of bleomycin as our study and reported that a single intra-tracheal delivery of bleomycin led to an inflammatory process between Day 1 and Day 9 post-bleomycin and then transitioned from there into a fibrotic/repair phase during Day 10–21 post-bleomycin.[37] Considering the massive inflammation and lung tissue damage during acute lung injury, it is reasonable to speculate that pulmonary spinal afferents could be irritated by inflammatory cytokines or tissue damage-released endotoxins to trigger sympatho-excitation during acute lung injury. However, at later stages of lung injury, inflammation subsides, and stimulation of these spinal afferents may normalize. Therefore, it may be that both sympathetic activation and macrophage activation in the SG are necessary for generating spontaneous PVCs following acute lung injury.

This study has a number of limitations. First, from this study, we are unable to determine how lung injury leads to macrophage activation in the SG. As the primary injury occurred in the lung and not the SG, this likely occurred through circulating factors such as cytokines or extracellular vesicles.[38] Furthermore, we did not explore how M1 macrophage activation sensitize SG neurons in vivo and in vitro. A likely mechanism is through release of cytokines to sensitize SG neurons via downstream inflammatory signaling pathways. It is

also possible that macrophages sensitized SGs through a non-cytokine-dependent mechanism. Interestingly, after SG neurons were co-cultured with macrophages overnight, the DiI dye in DiI-positive SG neurons leaked into the macrophages which were physically attached to SG neurons (Figure 7), indicating a potential cell-to-cell communication between SG neurons and their attached macrophages. Second, our bleomycin model might potentially limit the ability to broadly translate our study findings into clinical care of humans because the clinical aetiology of lung injury is variable. The most two common models to study lung injury are bleomycin and LPS models. However, as LPS has been shown to directly affect sympathetic and parasympathetic ganglia in addition to its effect on the lung itself,[39–43] the bleomycin model is more suitable for our current study, because our goal was to examine the lung injury-induced *secondary* neuronal dysfunction in SG. Third, we performed unilateral SG electrical stimulation rather than bilateral. Evidence from human studies[44–46] suggest that both left and right SG maybe involved in arrhythmogenesis. We could have compared the effect of left versus right versus bilateral electrical SG stimulation on PVCs in our experiments. However, this was in excess of our current study goals. Fourth, we did not assess the effects of bleomycin lung injury upon intracardiac ganglia, nor the contribution of intracardiac ganglia upon arrhythmogenesis in our model. However, it is possible that alterations in intracardiac ganglia in response to lung injury contribute to arrhythmogenesis. Additional investigation will be required to determine the role of intracardiac ganglia.

3.1 | Physiological relevance

Our study demonstrated a time-dependent macrophage activation in SG after a single tracheal instillation of bleomycin, which contributes to (a) the pathogenesis of cardiac arrhythmia in the acute lung injury state and (b) an increased vulnerability in triggering cardiac arrhythmia in the chronic lung injury state. A schematic diagram (Figure 8) briefly described our major findings in the SG post-lung injury. We believe that these findings could be useful to explain the underlying mechanisms of cardiac co-morbidity in chemical or infection-induced acute lung injury as well as chronic lung injury such as COPD. Our study also suggest that macrophage activation in SG has a priming effect on SG neurons rather than directly activating them. In addition to acute/chronic lung injury, stellate macrophage activation could also occur in non-pulmonary aetiology of cardiac arrhythmia. Therefore, macrophage activation in SG might be a potential new therapeutic target to treat cardiac arrhythmia in cardiopulmonary diseases.

4 | METHODS AND MATERIALS

All animal experimentation was approved by the Institutional Animal Care and Use Committee of the University of Nebraska Medical Center and was performed in accordance with the National Institutes of Health Guide for the Care and Use of Laboratory Animals. Experiments were performed on male, 2-month-old Sprague-Dawley rats (~300 g) purchased from Charles River Laboratories. Animals were housed on-site and allowed a 1-week acclimation prior to experiments. The rats were supplied with food and water ad libitum, and maintained on 12:12-hour light-dark cycles. A small number of rats (two sham rats and four bleomycin rats) were lost during experimentation because of telemetry unit failure (eg expired battery) or death stemming from severe lung injury. All animal

experimentation (eg electrical stimulation of the SG) was performed during the day, with the exception of radiotelemetry collection which occurred over 24 hours. Delivery of bleomycin (or saline), telemetry implantation, telemetry recordings and DiI delivery were performed within our animal housing centre. All other experiments were performed in our basic science lab.

4.1 | Drugs and chemicals

Bleomycin sulphate was purchased from Enzo Life Sciences (New York, USA). Bleomycin (2.5 mg/kg)[37] was dissolved in saline for intra-tracheal administration. This procedure was performed within the animal housing centre. Minocycline (20 mg/kg/d, Sigma-Aldrich)[47] was dissolved in drinking water. We monitored the volume of water ingested by each rat and adjusted the minocycline concentration accordingly to achieve the desired dose. Minocycline was selected as an experimental agent primarily because it has shown efficacy in reducing macrophage activation.[48,49] Thus, with minocycline, we are able to test the hypothesis that macrophage activation in the SG contributes to arrhythmogenesis following lung injury.

4.2 | Rat model of lung injury

Rats were randomized into three groups and evaluated at four time points (Week 1, 2, 3 and 4) post-instillation as follows: sham rats (n = 55), bleomycin-exposed rats without minocycline (n = 51) and bleomycin-exposed rats with minocycline treatment (n = 19). Minocycline treatment began 3 days prior to bleomycin instillation. Bleomycin (2.5 mg/kg, ~0.15 mL) was instilled intra-tracheally to the lungs under 3% isoflurane anaesthesia. Sham control underwent intra-tracheal instillation of saline. A brief experimental design protocol is also shown in Figures S1 and S2.

4.3 | Electrocardiographic (ECG) analysis

Two weeks before performing lung injury, the rats were implanted with ECG telemetry units (CTA-F40, Data Sciences International, St Paul, MN, USA). The rats were allowed to recover for 1 week, after which one 24-hour baseline recording was collected. Following lung injury, 24-hour ECG recordings were collected biweekly until euthanasia. ECG signals were digitized at a sampling frequency of 1 kHz using a PowerLab data acquisition system (ADInstruments, Colorado Springs, CO). The ECG analysis module in the LabChart 8 software (ADInstruments, Castle Hill, NSW, Australia) was used to visualize individual ECG signals. P wave, QRS complex and T waves were identified for individual ECG waveforms, and then all experimental ECG traces were analysed. The following parameters were determined: heart rate, P-wave duration, PR interval, QRS interval, QT interval and QT corrected for HR (QTc) using Bazett's formula.[50] Movement artefacts and electrical noise were identified on the ECG and eliminated from analysis. ECG recordings were quantified by the LabChart 8 software and are reported as per-hour averages and as 24-hour averages. Ventricular arrhythmias were recorded and analysed by an experienced researcher who was blinded to the group design. The occurrence of PVCs and AV block was quantified based on the Lambeth Conventions for the study of experimental arrhythmias.[51] The results of PVCs and AV block are reported as number of events per day.

4.4 | Heart rate variability measurements

To elucidate the potential mechanisms by which acute lung injury induces spontaneous cardiac arrhythmias, we evaluated autonomic function by HRV analysis. HRV has been reported to be an attractive, non-invasive method to study cardiac autonomic activity.[29] We measured the time and frequency domains of HRV by the SDRR and LF/HF, respectively. HRV analysis was conducted in the present study using LabChart 8 software. Initially, cardiotachograms were inspected to ensure that all R waves were correctly detected. Tachograms with ectopic beats and artefacts were discarded without substitution and excluded from further analysis. For time-domain analysis of HRV, the SDRR was calculated to represent overall HRV. For frequency-domain analysis, tachograms were resampled to equal intervals by the spline cubic interpolation method at 10 Hz, and the linear trend was removed. The power spectrum was obtained with a fast Fourier transform based method (Welch's periodogram: 256 points, 50% overlap and Hamming window).[52] Based on previously published studies in rats,[53–55] frequency-domain density was integrated in very low-frequency (VLF: 0–0.2 Hz), low-frequency (LF: 0.20–0.75 Hz) and high-frequency (HF: 0.75–3.0 Hz) bands. Power (in ms^2) was estimated as the area under the spectrum within these frequency ranges. The LF/HF was calculated to estimate sympatho-vagal balance. Time-domain (SDRR) and frequency-domain (LF/HF) parameters of HRV were then quantified and are reported as per-hour and per 24-hour averages.[56]

All telemetry recordings were 24 hours in length. These 24-hour recordings were divided into 24, 1-hour blocks for analysis. Reduction of ECG signal quality caused by movement artefacts and electrical noise were identified manually (with user judgement) and *not* included in the analysis. The ECG signal had to meet the following quality criteria in order to be included in analysis: (a) stable baseline signal, (b) no measurement discontinuities, (c) no movement artefacts and (d) stationary and high-quality ECG signal with clear R peaks.[57,58]

4.5 | Electrical stimulation of the decentralized SG

Minocycline was systemically administrated in the in vivo experiments. To differentiate a local effect of minocycline on the SG from a potential central effect, we performed direct electrical stimulation of the decentralized SG (which only contains the cardiac efferent nerve branch) to evaluate the local effect of minocycline on the SG. Under 2% isoflurane anaesthesia, rats were placed on a metal heating pad in the supine position. A small incision on the skin of anterior chest wall was made in the area below right collarbone. The right SG was identified aside the first thoracic vertebrae and disassociated from the adjacent tissues. The fibres of SG connecting to middle cervical ganglion and other ganglia were cut, while the branch to heart was preserved. A silver bipolar electrode was placed on the SG, and intermittent square wave pulses (5 V, 1 ms, 0.5–7 Hz for 30 seconds) were delivered by a pulse generator (model no. A310, WPI; Sarasota, FL). During the experiment, the rats were kept warm using an isothermal pad and heat lamp, while the SGs were moisturized by periodic administration of warm saline. Once the functional assessment was completed, rats were killed with an overdose of pentobarbital sodium (150 mg/kg, IV). This experimented was performed in our basic science laboratory.

4.6 | Histological examination

Sham and bleomycin rats (n = 3–4/group) were anesthetized with pentobarbital sodium (40 mg/kg, IP) and perfused through the aorta, first with phosphate-buffered saline (PBS; pH = 7.4) followed by 4% paraformaldehyde (in 0.1 mol/L PBS). The SG, heart and lung were immediately removed and immersed in the 4% paraformaldehyde solution overnight at 4°C. Heart and lung were dehydrated through a gradient series of alcohol, cleared in xylene and embedded in paraffin, cut into sections at 5 μm using a Leica rotary microtome. The SGs were dehydrated with 30% sucrose in PBS overnight, sectioned at 14 μm using a Leica cryostat (−20°C).

4.7 | Histological examination of lungs and heart

After being rehydrated, heart and lung sections (5 μm thick) were stained with Masson-Trichrome and CD3 antibody (1:150, ab16669, Abcam, Cambridge, MA, USA). High-resolution digital images (40× objective) of entire heart or lung sections were scanned in the tissue core facility at the University of Nebraska Medical Center.

4.8 | Immunofluorescence staining of SG

Double immunostaining of ionized calcium-binding adaptor molecule 1 (Iba1, a macrophage marker) with tyrosine hydroxylase (TH, a sympathetic neuronal marker) was performed by pre-incubation of 10% donkey serum for 60 minutes and then incubated with rabbit anti-Iba1 antibody (1:200 dilution, NBP2–19019, Novus Biologicals, Littleton, CO, USA) and sheep anti-TH antibody (1:500 dilution, NB300–110, Novus Biologicals) overnight at 4°C. Sections were then washed with PBS and incubated with fluorescence-conjugated secondary antibody (Alexa 594-conjugated donkey anti-rabbit IgG and Alexa 488-conjugated donkey anti-Sheep, 1:200, Invitrogen, CA, USA) for 1 hour at room temperature. Slides were covered by UltraCruz aqueous mounting medium with 4′,6-diamidino-2-phenylindole (DAPI, sc24941, Santa Cruz, CA, USA) observed on a laser confocal microscope (Leica TCS STED, Leica Microsystems Inc, Buffalo Grove, IL, USA), and images captured using a digital camera system. No staining was seen when a negative control was performed with PBS instead of the primary antibody.

Three or four non-consecutive sections per rat that contains similar number of TH-positive neurons were chosen and Iba1-positive (macrophages) cells were counted in a region of interest (ROI) of 150 × 150 μm^2 per section using Image-Pro Plus software 6.0 (Media Cybernetics Inc, Rockville, USA). Finally, the number of Iba1-positive cells in the ROI from 12 to 14 sections per group were averaged and reported as mean number per group.

4.9 | Western blot

Western blots were performed to measure the relative protein expression of IRF8 (a critical regulatory factor for pro-inflammatory macrophage/microglia activation)[15,16] in resected SG at the different time points post-bleomycin instillation. In preparation for Western blot, bilateral SGs were processed using a lysis buffer made from a 100:1 dilution of radioimmunoprecipitation (RIPA) buffer and a protease inhibitor cocktail (Sigma-Aldrich, Atlanta, GA, USA). This mixture was then homogenized, centrifuged and stored at −80°C until use. Protein concentration was measured by the BCA protein assay method using

bovine serum albumin (BSA) as standard (Thermo Scientific). The proteins were loaded onto a 10% SDS-PAGE gel along with protein standards (Bio-Rad Laboratories) in a separate lane for electrophoresis and then transferred to polyvinylidene fluoride membrane. The membrane was probed with mouse antibodies against IRF8 (1:500, Santa Cruz Biotechnology) and GAPDH (1:1000, Santa Cruz Biotechnology) and secondary antibody of goat anti-mouse (1:5000, Pierce Chemical). The protein signals were detected by enhanced chemiluminescence reagent (Pierce Chemical) and analysed using UVP BioImaging Systems. The densitometric result of IRF8 was reported as the ratio to GAPDH and then finally normalized to age-matched sham rats.

4.10 | DiI injection into heart

Male Sprague-Dawley rats were anaesthetized by inhalation of an isoflurane-oxygen mixture (3%−5% isoflurane in oxygen). After left thoracotomy, we injected the fluorescent retrograde tracer 1,1′-dioctadecyl-3,3,3′,3′-tetramethylindo carbocyanine percholate (DiI, 2 mg/mL; Molecular Probes, Eugene, OR, USA) sub-epicardially into both ventricles at basal, middle and apex sites (1 μL/per site) in order to retrogradely label cardiac SG neurons. Only DiI-labelled SG neurons (ie cardiac SG neurons) were recorded using the whole-cell patch-clamp technique. After DiI injection, the chest was closed followed by manual re-establishment of intrapleural pressure. Buprenorphine (0.05 mg/kg, SC) was given once immediately following surgery and on post-operative Days 1 and 2 for alleviation of pain. Rats returned to their cages for 4–5 days to allow transportation of the tracer to the SG neurons.

4.11 | Isolation of SG neurons

Rats were initially anesthetized with urethane (800 mg/kg, IP) and α-chloralose (40 mg/kg, IP) and then were killed with an overdose of pentobarbital sodium (150 mg/kg, IV). The SG dissociation protocol was kindly shared by Dr Runping Wang from the University of Iowa, which they used to dissociate nodose ganglia in previous studies.[59,60] In brief, bilateral SGs were removed and pooled, placed in Dulbecco's Modified Eagle Medium/Nutrient Mixture F-12 (DMEM/F12; Gibco, Carlsbad, CA, USA) containing 1% ITS Liquid Media Supplement and 1% Penicillin-Streptomycin. The SGs were mechanically triturated and incubated for 1 hour at 37°C in an enzymatic cocktail containing 0.1% collagenase/0.1% trypsin/0.01% DNase (Worthington, Indiana, USA). The cell suspension was diluted with medium containing 0.1% BSA and 0.01 mol/L HEPES and was centrifuged. The dispersed SG cells were resuspended in DMEM containing 1% Penicillin-Streptomycin and plated onto culture wells.

4.12 | Co-culture of SG neurons with LPS-activated RAW264.7 macrophages

The RAW264.7 cell line was purchased from ATCC (TIB-71, Manassas, VA, USA) and was cultured in DMEM (high glucose, no HEPES) supplemented with 10% FBS. The RAW264.7 macrophage cells were seeded (1×10^5 cells/cm^2) at T-25 flask overnight and pretreatment with lipopolysaccharide (LPS; 25 ng/mL) for 4 hours. Immediately after the SG neurons were isolated, the LPS-pretreated RAW264.7 cell suspension was added into the SG neuron medium. The final ratio of SG neurons to macrophages was approximately 1:10.

All cells were cultured overnight at 37°C in a humidified atmosphere of 95% air 5% CO_2 before the patch-clamp experiments.

4.13 | Electrophysiological recordings

APs were recorded using the whole-cell patch-clamp technique using the Axopatch 200B patch-clamp amplifier (Axon Instruments, Burlingame, CA, USA) as previously described.[61] Only DiI-labelled SG neurons were recorded. APs were elicited by a ramp current injection of 0–100 pA. The current threshold-induced APs or threshold potential was measured at the beginning of the first AP. The frequency of APs was measured in a 1-s current clamp (10-pA step decrements from 0 to 60 nA for 1 seconds). The patch pipette solution was composed of (in mmol/L) 105 K-aspartate, 20 KCl, 1 $CaCl_2$, 5 MgATP, 10 HEPES, 10 EGTA and 25 glucose (pH 7.2; 320 mosM). The bath solution was composed of (in mmmol/L) 140 NaCl, 5.4 KCl, 0.5 $MgCl_2$, 2.5 $CaCl_2$, 5.5 HEPES, 11 glucose and 10 sucrose (pH 7.4; 330 mosM). The pCLAMP 10.2 program (Axon Instruments, San Jose, CA, USA) was used for data acquisition and analysis. All experiments were done at room temperature (22–24°C).

4.14 | Statistical analysis

All values are expressed as mean ± SD. The Shapiro-Wilk test was used for assessing distribution. The unpaired two-tailed Student's *t* test and a two-way ANOVA were used for data that were normally distributed, and the Mann-Whitney *U* test was used for data that were not normally distributed. Counts of electrical stimulation-induced PVCs at different frequencies and APs at different injected currents were analysed with repeated measures ANOVA. Because of the length (4 weeks) of the study, some telemetry data sets contained some missing values that were missing at random, and a mixed-effects model for repeated measures ANOVA was used when we were analysing telemetry data including number of PVCs and AV blocks, HRV data and ECG parameters. Statistical significance was considered to be at a *P*-value < .05. All statistical analyses and graphs were made using GraphPad Prism 8 (GraphPad Software, San Diego, CA).

Supplementary Material

Refer to Web version on PubMed Central for supplementary material.

ACKNOWLEDGEMENTS

We sincerely thank Dr Runping Wang (PhD, from Department of Internal Medicine, University of Iowa, Iowa City, Iowa, USA) to share her NG/SG dissociation protocol. Without her critical support, we would not have completed the patch-clamp experiments in this study.

Funding information

This study was supported by NIH grant 1R01 HL-152160 and partially supported by 2R01 HL126796 and 1R01 HL-121012. Dr Hanjun Wang is also supported by Margaret R. Larson Professorship in Anesthesiology. Dr Irving H. Zucker is supported in part by the Theodore F. Hubbard Professorship for Cardiovascular Research.

REFERENCES

1. Dyszkiewicz W, Skrzypczak M. Atrial fibrillation after surgery of the lung: clinical analysis of risk factors. Eur J Cardiothorac Surg. 1998;13(6):625–628. [PubMed: 9686791]
2. Shih HT, Webb CR, Conway WA, Peterson E, Tilley B, Goldstein S. Frequency and significance of cardiac arrhythmias in chronic obstructive lung disease. Chest. 1988;94(1):44–48. [PubMed: 2454781]
3. Amar D, Zhang H, Roistacher N. The incidence and outcome of ventricular arrhythmias after noncardiac thoracic surgery. Anesth Analg. 2002;95(3):537–543, table of contents. [PubMed: 12198031]
4. Sode BF, Dahl M, Nordestgaard BG. Myocardial infarction and other co-morbidities in patients with chronic obstructive pulmonary disease: a Danish nationwide study of 7.4 million individuals. Eur Heart J. 2011;32(19):2365–2375. [PubMed: 21875856]
5. Fontecave Jallon J, Abdulhay E, Calabrese P, Baconnier P, Gumery PY. A model of mechanical interactions between heart and lungs. Philos Trans A Math Phys Eng Sci. 1908;2009(367):4741–4757.
6. Bouferrache K, Vieillard-Baron A. Acute respiratory distress syndrome, mechanical ventilation, and right ventricular function. Curr Opin Crit Care. 2011;17(1):30–35. [PubMed: 21157319]
7. Gordo-Vidal F, Enciso-Calderon V. Acute respiratory distress syndrome, mechanical ventilation and right ventricular function. Med Intensiva. 2012;36(2):138–142. [PubMed: 21999947]
8. Grubler MR, Wigger O, Berger D, Blochlinger S. Basic concepts of heart-lung interactions during mechanical ventilation. Swiss Med Wkly. 2017;147:w14491. [PubMed: 28944931]
9. Vaseghi M, Shivkumar K. The role of the autonomic nervous system in sudden cardiac death. Prog Cardiovasc Dis. 2008;50(6):404–419. [PubMed: 18474284]
10. Zipes DP, Barber MJ, Takahashi N, Gilmour RF Jr. Influence of the autonomic nervous system on the genesis of cardiac arrhythmias. Pacing Clin Electrophysiol. 1983;6(5 Pt 2):1210–1220. [PubMed: 6195641]
11. Ajijola OA, Lellouche N, Bourke T, et al. Bilateral cardiac sympathetic denervation for the management of electrical storm. J Am Coll Cardiol. 2012;59(1):91–92. [PubMed: 22192676]
12. Vaseghi M, Gima J, Kanaan C, et al. Cardiac sympathetic denervation in patients with refractory ventricular arrhythmias or electrical storm: intermediate and long-term follow-up. Heart Rhythm. 2014;11(3):360–366. [PubMed: 24291775]
13. Vaseghi M, Barwad P, Malavassi Corrales FJ, et al. Cardiac sympathetic denervation for refractory ventricular arrhythmias. J Am Coll Cardiol. 2017;69(25):3070–3080. [PubMed: 28641796]
14. Rizzo S, Basso C, Troost D, et al. T-cell-mediated inflammatory activity in the stellate ganglia of patients with ion-channel disease and severe ventricular arrhythmias. Circ Arrhythm Electrophysiol. 2014;7(2):224–229. [PubMed: 24532560]
15. Masuda T, Tsuda M, Yoshinaga R, et al. IRF8 is a critical transcription factor for transforming microglia into a reactive phenotype. Cell Rep. 2012;1(4):334–340. [PubMed: 22832225]
16. Langlais D, Barreiro LB, Gros P. The macrophage IRF8/IRF1 regulome is required for protection against infections and is associated with chronic inflammation. J Exp Med. 2016;213(4):585–603. [PubMed: 27001747]
17. Restrepo MI, Reyes LF. Pneumonia as a cardiovascular disease. Respirology. 2018;23(3):250–259. [PubMed: 29325222]
18. Hudson LD. Significance of arrhythmias in acute respiratory failure. Geriatrics. 1976;31(11):61–64.
19. Kusunoki Y, Nakamura T, Hattori K, et al. Atrial and ventricular arrhythmia-associated factors in stable patients with chronic obstructive pulmonary disease. Respiration. 2016;91(1):34–42. [PubMed: 26695820]
20. Moeller A, Ask K, Warburton D, Gauldie J, Kolb M. The bleomycin animal model: a useful tool to investigate treatment options for idiopathic pulmonary fibrosis? Int J Biochem Cell Biol. 2008;40(3):362–382. [PubMed: 17936056]

21. Comazzi R, Misrachi D, Galimberti M, Piva L, Pizzoccaro G, Villani F. Detection of cardiac arrhythmias and ischaemic events in combination chemotherapy with cisplatin, etoposide and bleomycin for testicular cancer. Anticancer Res. 1989;9(3):663–665. [PubMed: 2475052]
22. Villani F, Misrachi D, Galimberti M. Cardiac arrhythmia and ischaemic events after combination chemotherapy for testicular cancer. Eur Heart J. 1994;15(11):1533–1536. [PubMed: 7530660]
23. Sheldon SH, Gard JJ, Asirvatham SJ. Premature ventricular contractions and non-sustained ventricular tachycardia: association with sudden cardiac death, risk stratification, and management strategies. Indian Pacing Electrophysiol J. 2010;10(8):357–371. [PubMed: 20811538]
24. Wang HJ, Wang W, Cornish KG, Rozanski GJ, Zucker IH. Cardiac sympathetic afferent denervation attenuates cardiac remodeling and improves cardiovascular dysfunction in rats with heart failure. Hypertension. 2014;64(4):745–755. [PubMed: 24980663]
25. Fukuda K, Kanazawa H, Aizawa Y, Ardell JL, Shivkumar K. Cardiac innervation and sudden cardiac death. Circ Res. 2015;116(12):2005–2019. [PubMed: 26044253]
26. Wang HJ, Rozanski GJ, Zucker IH. Cardiac sympathetic afferent reflex control of cardiac function in normal and chronic heart failure states. J Physiol. 2017;595(8):2519–2534. [PubMed: 28116751]
27. Coleman B, Worthen MC, McCanon DM, Kallal JE, Luisada AA. Sympathetic influence on ventricular compliance. Jpn Heart J. 1976;17(2):222–232. [PubMed: 933360]
28. Olde Nordkamp LR, Driessen AH, Odero A, et al. Left cardiac sympathetic denervation in the Netherlands for the treatment of inherited arrhythmia syndromes. Neth Heart J. 2014;22(4):160–166. [PubMed: 24522951]
29. Shen MJ, Zipes DP. Role of the autonomic nervous system in modulating cardiac arrhythmias. Circ Res. 2014;114(6):1004–1021. [PubMed: 24625726]
30. Zipes DP. Antiarrhythmic therapy in 2014: contemporary approaches to treating arrhythmias. Nat Rev Cardiol. 2015;12(2):68–69. [PubMed: 25533797]
31. Buckley U, Yamakawa K, Takamiya T, Andrew Armour J, Shivkumar K, Ardell JL. Targeted stellate decentralization: implications for sympathetic control of ventricular electrophysiology. Heart Rhythm. 2016;13(1):282–288. [PubMed: 26282244]
32. Irie T, Yamakawa K, Hamon D, Nakamura K, Shivkumar K, Vaseghi M. Cardiac sympathetic innervation via middle cervical and stellate ganglia and antiarrhythmic mechanism of bilateral stellectomy. Am J Physiol Heart Circ Physiol. 2017;312(3):H392–H405. [PubMed: 28011590]
33. Xu H, Zhu J, Smith S, et al. Notch-RBP-J signaling regulates the transcription factor IRF8 to promote inflammatory macrophage polarization. Nat Immunol. 2012;13(7):642–650. [PubMed: 22610140]
34. Jacono FJ, Peng YJ, Nethery D, et al. Acute lung injury augments hypoxic ventilatory response in the absence of systemic hypoxemia. J Appl Physiol. 2006;101(6):1795–1802. [PubMed: 16888052]
35. Cao Z, Lis R, Ginsberg M, et al. Targeting of the pulmonary capillary vascular niche promotes lung alveolar repair and ameliorates fibrosis. Nat Med. 2016;22(2):154–162. [PubMed: 26779814]
36. Shanks J, Xia Z, Lisco SJ, et al. Sympatho-excitatory response to pulmonary chemosensitive spinal afferent activation in anesthetized, vagotomized rats. Physiol Rep. 2018;6(12):e13742. [PubMed: 29906340]
37. Chaudhary NI, Schnapp A, Park JE. Pharmacologic differentiation of inflammation and fibrosis in the rat bleomycin model. Am J Respir Crit Care Med. 2006;173(7):769–776. [PubMed: 16415276]
38. Hood JL, San RS, Wickline SA. Exosomes released by melanoma cells prepare sentinel lymph nodes for tumor metastasis. Cancer Res. 2011;71(11):3792–3801. [PubMed: 21478294]
39. Boucher Y, Moreau N, Mauborgne A, Dieb W. Lipopolysaccharide-mediated inflammatory priming potentiates painful post-traumatic trigeminal neuropathy. Physiol Behav. 2018;194:497–504. [PubMed: 29928887]
40. Kunda PE, Cavicchia JC, Acosta CG. Lipopolysaccharides and trophic factors regulate the LPS receptor complex in nodose and trigeminal neurons. Neuroscience. 2014;280:60–72. [PubMed: 25218806]

41. Hosoi T, Okuma Y, Matsuda T, Nomura Y. Novel pathway for LPS-induced afferent vagus nerve activation: possible role of nodose ganglion. Auton Neurosci. 2005;120(1–2):104–107. [PubMed: 15919243]
42. Shadiack AM, Carlson CD, Ding M, Hart RP, Jonakait GM. Lipopolysaccharide induces substance P in sympathetic ganglia via ganglionic interleukin-1 production. J Neuroimmunol. 1994;49(1–2):51–58. [PubMed: 7507497]
43. Blum E, Procacci P, Conte V, Sartori P, Hanani M. Long term effects of lipopolysaccharide on satellite glial cells in mouse dorsal root ganglia. Exp Cell Res. 2017;350(1):236–241. [PubMed: 27914789]
44. Fujiki A, Masuda A, Inoue H. Effects of unilateral stellate ganglion block on the spectral characteristics of heart rate variability. Jpn Circ J. 1999;63(11):854–858. [PubMed: 10598890]
45. Randall WC, Rohse WG. The augmentor action of the sympathetic cardiac nerves. Circ Res. 1956;4(4):470–475. [PubMed: 13330193]
46. Rogers MC, Battit G, McPeek B, Todd D. Lateralization of sympathetic control of the human sinus node: ECG changes of stellate ganglion block. Anesthesiology. 1978;48(2):139–141. [PubMed: 655444]
47. Hinwood M, Morandini J, Day TA, Walker FR. Evidence that microglia mediate the neurobiological effects of chronic psychological stress on the medial prefrontal cortex. Cereb Cortex. 2012;22(6):1442–1454. [PubMed: 21878486]
48. Aceves M, Terminel MN, Okoreeh A, et al. Morphine increases macrophages at the lesion site following spinal cord injury: Protective effects of minocycline. Brain Behav Immun. 2019;79:125–138. [PubMed: 30684649]
49. Gu C, Hao X, Li J, Hua Y, Keep RF, Xi G. Effects of minocycline on epiplexus macrophage activation, choroid plexus injury and hydrocephalus development in spontaneous hypertensive rats. J Cereb Blood Flow Metab. 2019;39(10):1936–1948. [PubMed: 30862302]
50. Indik JH, Pearson EC, Fried K, Woosley RL. Bazett and Fridericia QT correction formulas interfere with measurement of drug-induced changes in QT interval. Heart Rhythm. 2006;3(9):1003–1007. [PubMed: 16945790]
51. Curtis MJ, Hancox JC, Farkas A, et al. The Lambeth Conventions (II): guidelines for the study of animal and human ventricular and supraventricular arrhythmias. Pharmacol Ther. 2013;139(2):213–248. [PubMed: 23588158]
52. Welch PD. The use of fast Fourier transforms for the estimation of power spectra: a method based on time averaging over short modified periodograms. IEEE Trans Audio Electroacoust. 1967;15:70–73.
53. Souza HC, De Araujo JE, Martins-Pinge MC, Cozza IC, Martins-Dias DP. Nitric oxide synthesis blockade reduced the baroreflex sensitivity in trained rats. Auton Neurosci. 2009;150(1–2):38–44. [PubMed: 19443278]
54. Carnevali L, Sgoifo A. Vagal modulation of resting heart rate in rats: the role of stress, psychosocial factors, and physical exercise. Front Physiol. 2014;5:118. [PubMed: 24715877]
55. Silva LEV, Geraldini VR, de Oliveira BP, Silva CAA, Porta A, Fazan R. Comparison between spectral analysis and symbolic dynamics for heart rate variability analysis in the rat. Sci Rep. 2017;7(1):8428. [PubMed: 28814785]
56. Carnevali L, Statello R, Sgoifo A. Resting heart rate variability predicts vulnerability to pharmacologically-induced ventricular arrhythmias in male rats. J Clin Med. 2019;8(5):655.
57. Rodrigues J, Belo D, Gamboa H. Noise detection on ECG based on agglomerative clustering of morphological features. Comput Biol Med. 2017;87:322–334. [PubMed: 28649031]
58. Patel SI, Souter MJ. Equipment-related electrocardiographic artifacts: causes, characteristics, consequences, and correction. Anesthesiology. 2008;108(1):138–148. [PubMed: 18156892]
59. Wang R, Lu Y, Gunasekar S, et al. The volume-regulated anion channel (LRRC8) in nodose neurons is sensitive to acidic pH. JCI Insight. 2017;2(5):e90632. [PubMed: 28289711]
60. Snitsarev V, Whiteis CA, Chapleau MW, Abboud FM. Mechano- and chemosensitivity of rat nodose neurones–selective excitatory effects of prostacyclin. J Physiol. 2007;582(Pt 1):177–194. [PubMed: 17478531]

61. Schiller AM, Hong J, Xia Z, Wang HJ. Increased brain-derived neurotrophic factor in lumbar dorsal root ganglia contributes to the enhanced exercise pressor reflex in heart failure. Int J Mol Sci. 2019;20(6):1480.

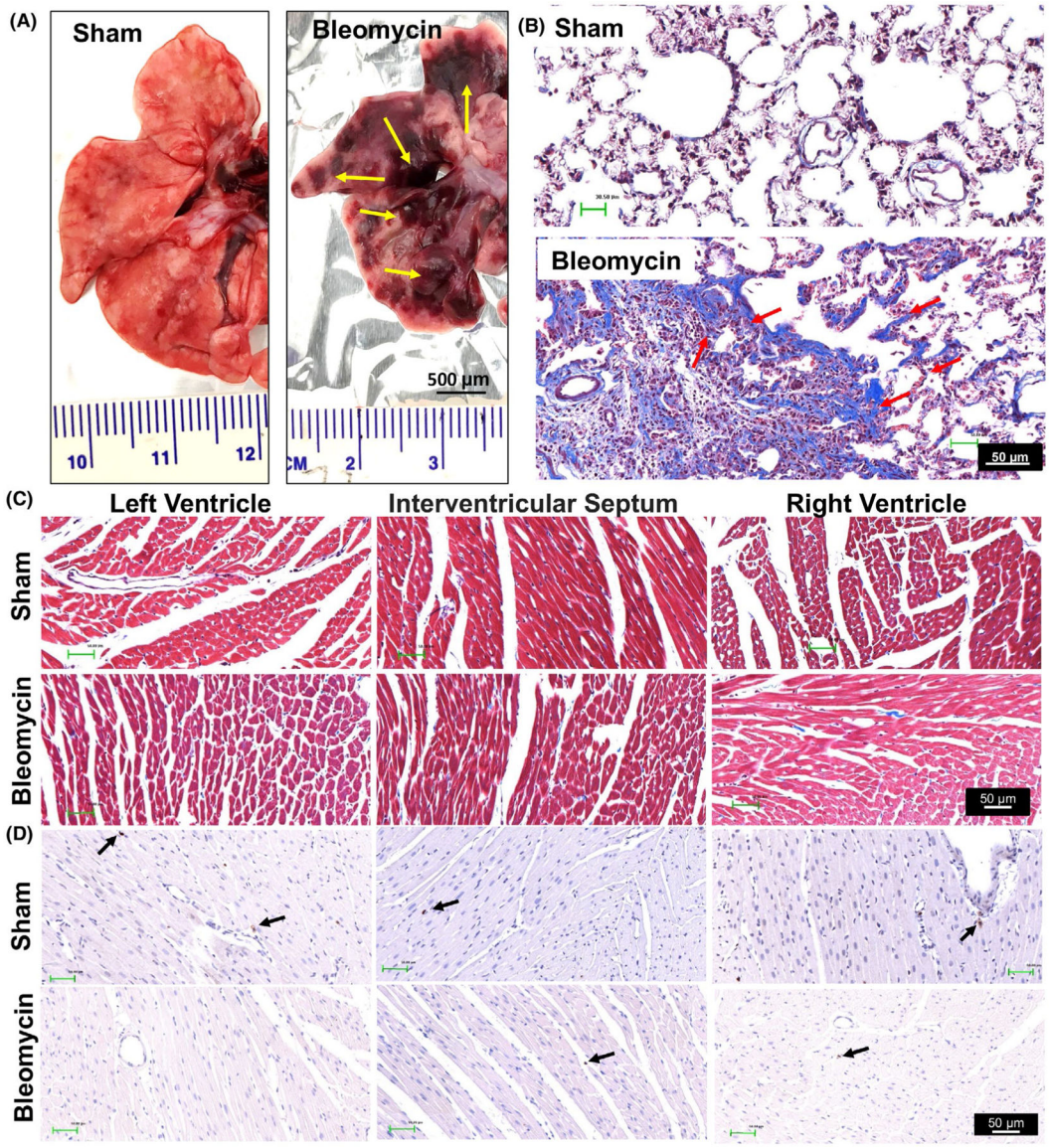

FIGURE 1.

Representative histological images showing lung injury (A) and (B) and the lack of injury/inflammation in the heart (C and D) at 2-week post-bleomycin injection. Yellow arrows in Panel A point to areas of lung injury induced by bleomycin. Scale bar = 500 μm. Red arrows in Panel B point to lung fibrosis area by Masson-Trichrome staining. Black arrows in Panel D point to T cells stained by the CD3 antibody. Scale bar = 50 μm. Cardiac histological images in Panel C and D indicate that no obvious cardiac fibrosis or T-cell infiltration was developed post-bleomycin. Scale bar = 50 μm. n = 3/each group

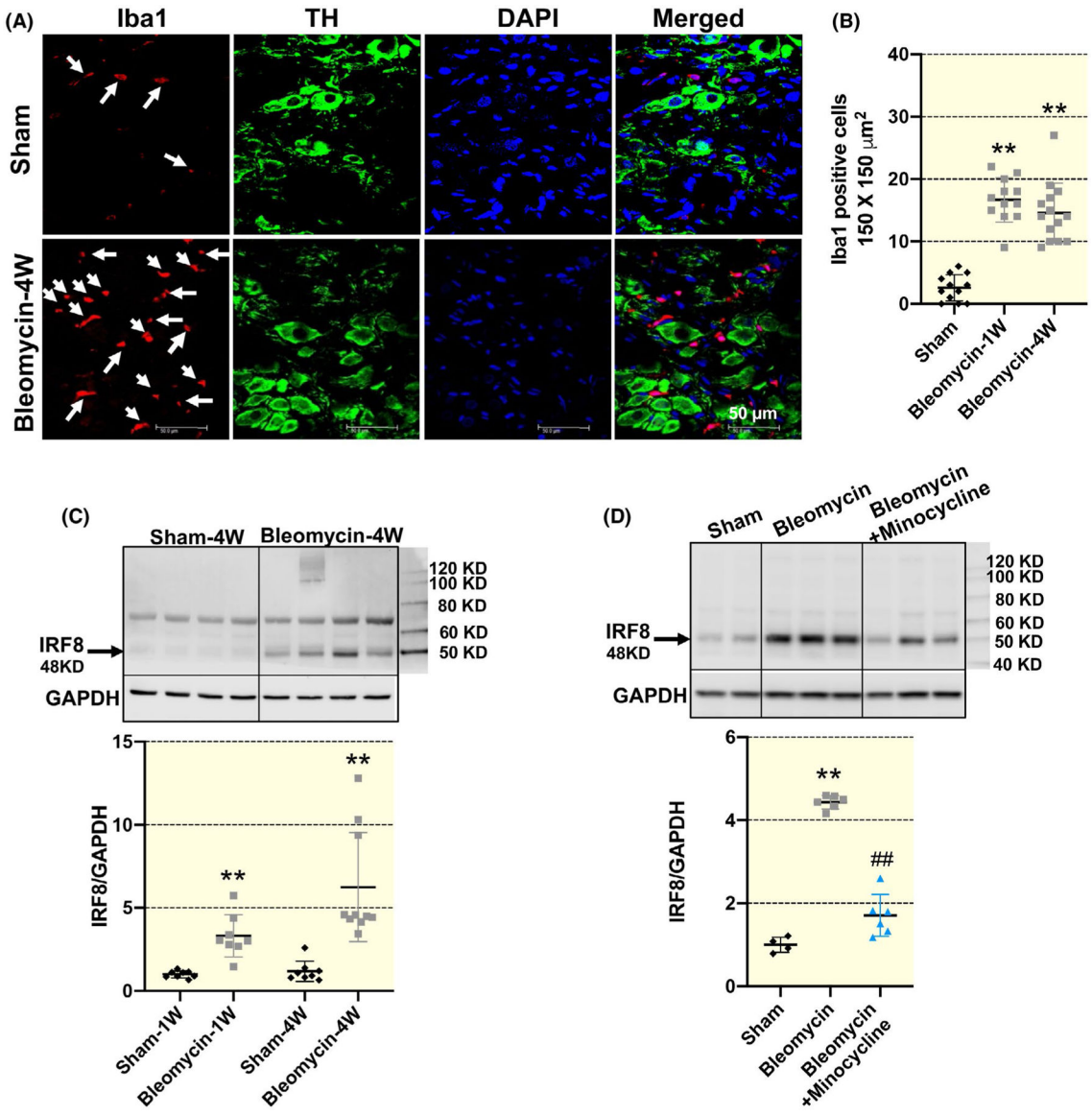

FIGURE 2.

Representative immunofluorescence images (A) and summary data (B) showing increased number of ionized calcium-binding adaptor molecule 1 (Iba1)-positive macrophages in the stellate ganglia (SG) in 1-week and 4-week bleomycin-treated rats compared with sham rats (n = 12 slices from four rats/sham and bleomycin group, n = 14 slices from four rats/ bleomycin + minocycline group). Scale bar = 50 μm. TH, tyrosine hydroxylase, a SG neuron marker; DAPI, a nuclear marker. Scale bar = 50 μm. White arrows point to the Iba1-positive macrophages (red) which do not co-localize with TH-positive SG neuron. ** $P < .01$ vs sham group. C, Representative Western blot images and mean data showing that IRF8 expression was time-dependently increased in the SGs of 1-week and 4-week bleomycin rats. n = 8/ sham-1w, sham-4w, bleomycin-1w group, n = 10/bleomycin-4w group. ** $P < .01$ versus age-matched sham group. D, Representative Western blot images and mean data showing that the increased protein expression of IRF8 in the SGs of 4-week bleomycin rats was

largely prevented by minocycline. Data are expressed as mean ± SD. n = 4/sham group, n = 6/bleomycin and bleomycin + minocycline group. $^{**}P < .01$ versus sham group. $^{\#\#}P < .01$ versus 4-wk bleomycin group

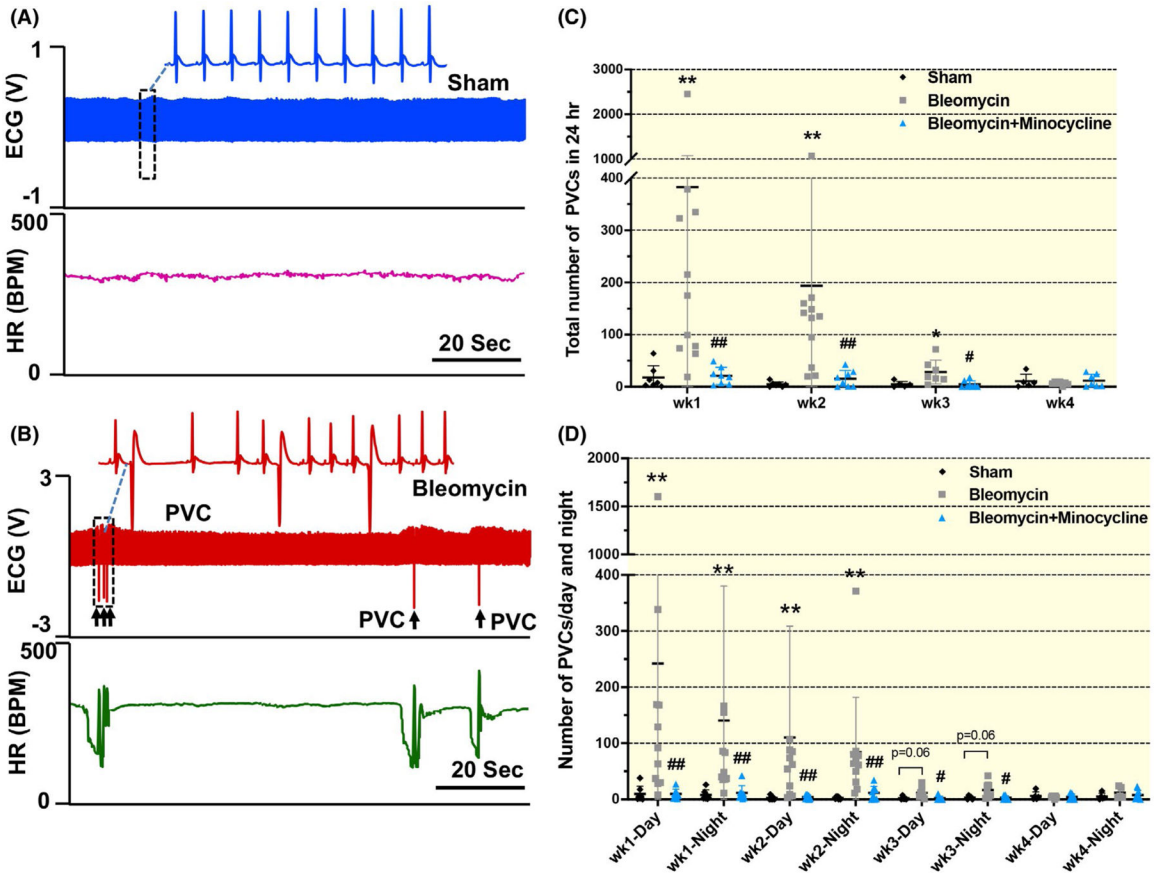

FIGURE 3.

Original tracing (A and B) and mean data (C and D) showing the number of premature ventricular contractions (PVCs) per 24 hours and their distributions over day and night in sham, bleomycin and bleomycin + minocycline rats at different time points (1, 2, 3 and 4 wk post-bleomycin). Scale bar = 20 sec. Data are expressed as mean ± SD. n = 7/sham, n = 11/bleomycin group, n = 8/bleomycin + minocycline group. $^{**}P < .01$ versus sham group. $^{\#}P < .05$ and $^{\#\#}P < .01$ versus bleomycin group

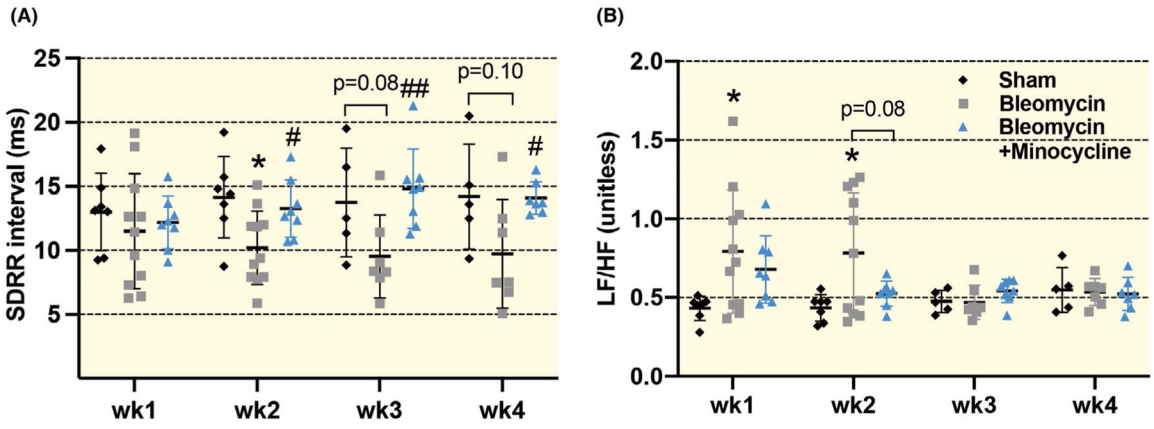

FIGURE 4.

Summarized data (A and B) showing the heart rate variability (HRV) parameters including the standard deviation of RR interval (SDRR) and low frequency/high frequency ratio (LF/HF) in sham, bleomycin and bleomycin + minocycline rats with different time points (1, 2, 3 and 4 wk post-bleomycin). Data are expressed as mean ± SD. n = 7/sham, n = 11/bleomycin group, n = 8/bleomycin + minocycline group. $^{*}P < .05$ versus sham group. $^{\#}P < .05$ and $^{\#\#}P < .01$ versus bleomycin group

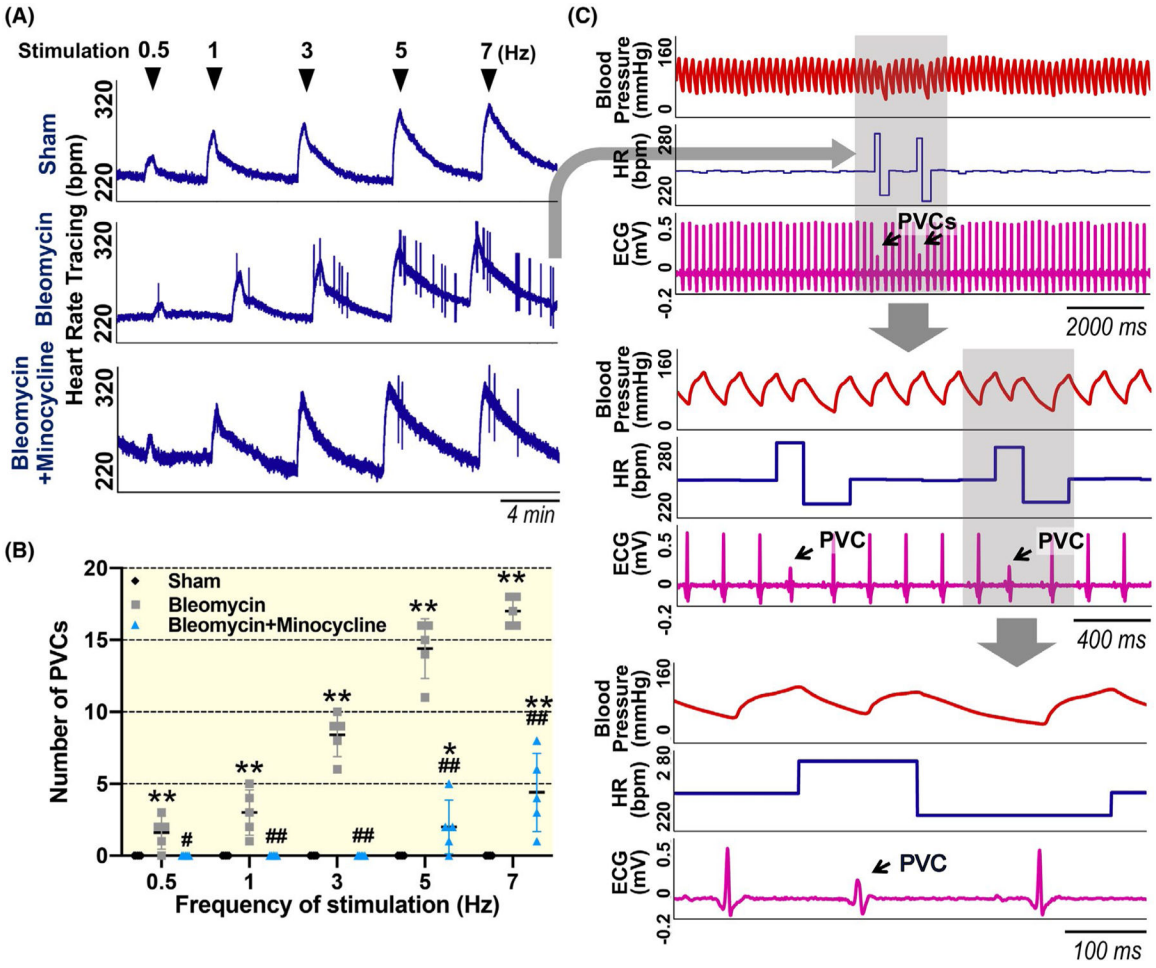

FIGURE 5.

Original tracings (A and C) and summary data (B) showing the number of premature ventricular contractions (PVCs) after electrical stimulation at different frequencies (0.5, 1, 3, 5 and 7 Hz) to the decentralized SG in 4 wk of sham, bleomycin and bleomycin + minocycline rats. Blue arrowheads indicate when electrical stimulation was administered. Black arrows in Panel C point to PVCs. Data are expressed as mean ± SD. n = 5/each group. $^{**}P < .001$ versus sham, $^{\#\#}P < .001$ versus bleomycin group. ECG, electrocardiogram; HR, heart rate; PVC, premature ventricular contraction

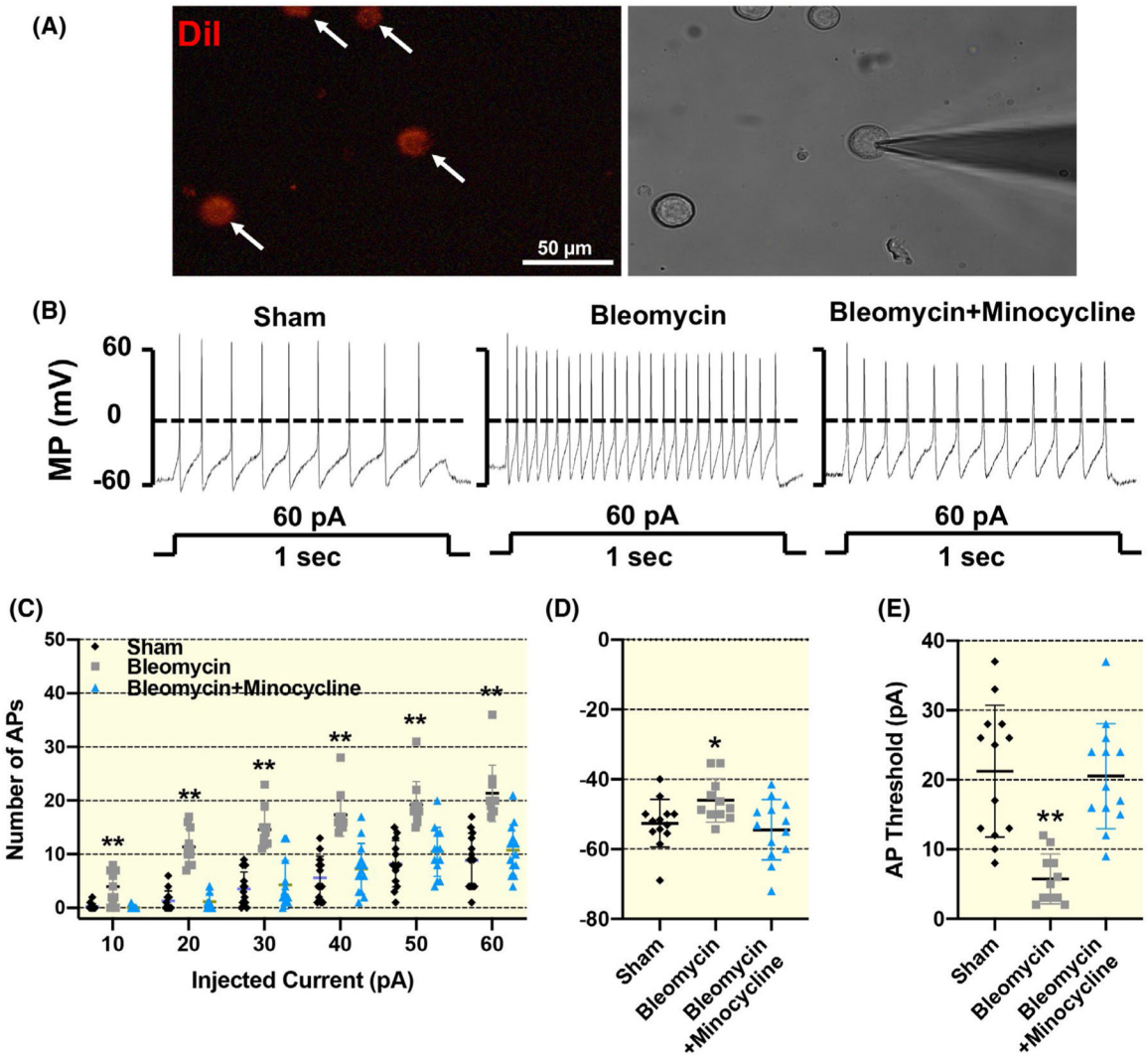

FIGURE 6.

Representative images (A and B) and summary data (C) showing increased SG neuronal excitability in 4 weeks of bleomycin rats, which was inhibited by chronic minocycline administration. A, Representative images showing how we identified cardiac efferents in the SG during patch-clamp experiments. Neuronal tracer DiI retrogradely labelled cardiac efferent SG neurons (white arrows) with red colour in fluorescent light (left) and cells in the same field under regular light. Scale bar = 50 μm. Original tracings (B) and mean data (C-E) showing action potential properties in response to both step and ramp current-injection protocols in the neuronal tracer DiI-labelled cardiac SG neurons from sham, bleomycin and bleomycin + minocycline rats. Data are expressed as mean ± SD. n = 13 neurons/sham, n = 11 neurons/bleomycin, n = 13 neurons/bleomycin + minocycline from six rats/each group. *P <.05 and **P <.01 versus both sham and bleomycin + minocycline groups

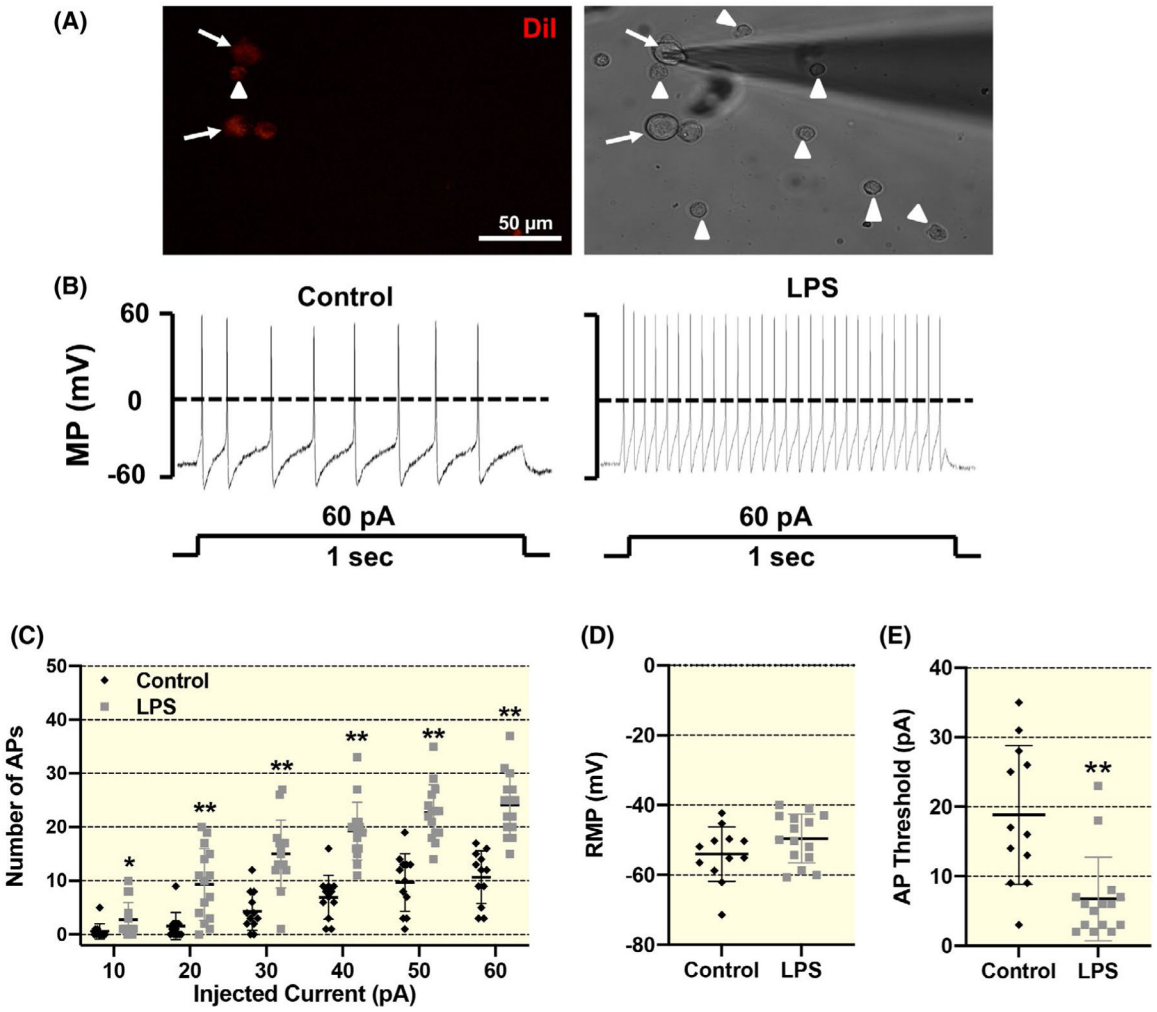

FIGURE 7.

Representative images and summary data showing the influence of macrophages on cardiac SG neurons in vitro. A, Representative images showing co-culture of neuronal tracer DiI-labelled cardiac SG neurons with lipopolysaccharide (LPS)-pretreated RAW264.7 macrophages during patch-clamp experiments. The DiI-labelled SG neurons are depicted by white arrow, and macrophages are shown by white arrowheads. Scale bar = 50 μm. B-E, original patch clamp tracings and mean data showing the action potential (AP) properties in response to both step and ramp current-injection protocols in DiI-labelled cardiac SG neurons following overnight co-culture with vehicle- or LPS-pretreated macrophages. Data are expressed as mean ± SD. n = 12 neurons from 6 rats/vehicle group, n = 15 neurons from eight rats/LPS-pretreated macrophages group. *P <.05 and **P <.01 versus control group. AP, action potential. MP, membrane potential; RMP, resting membrane potential

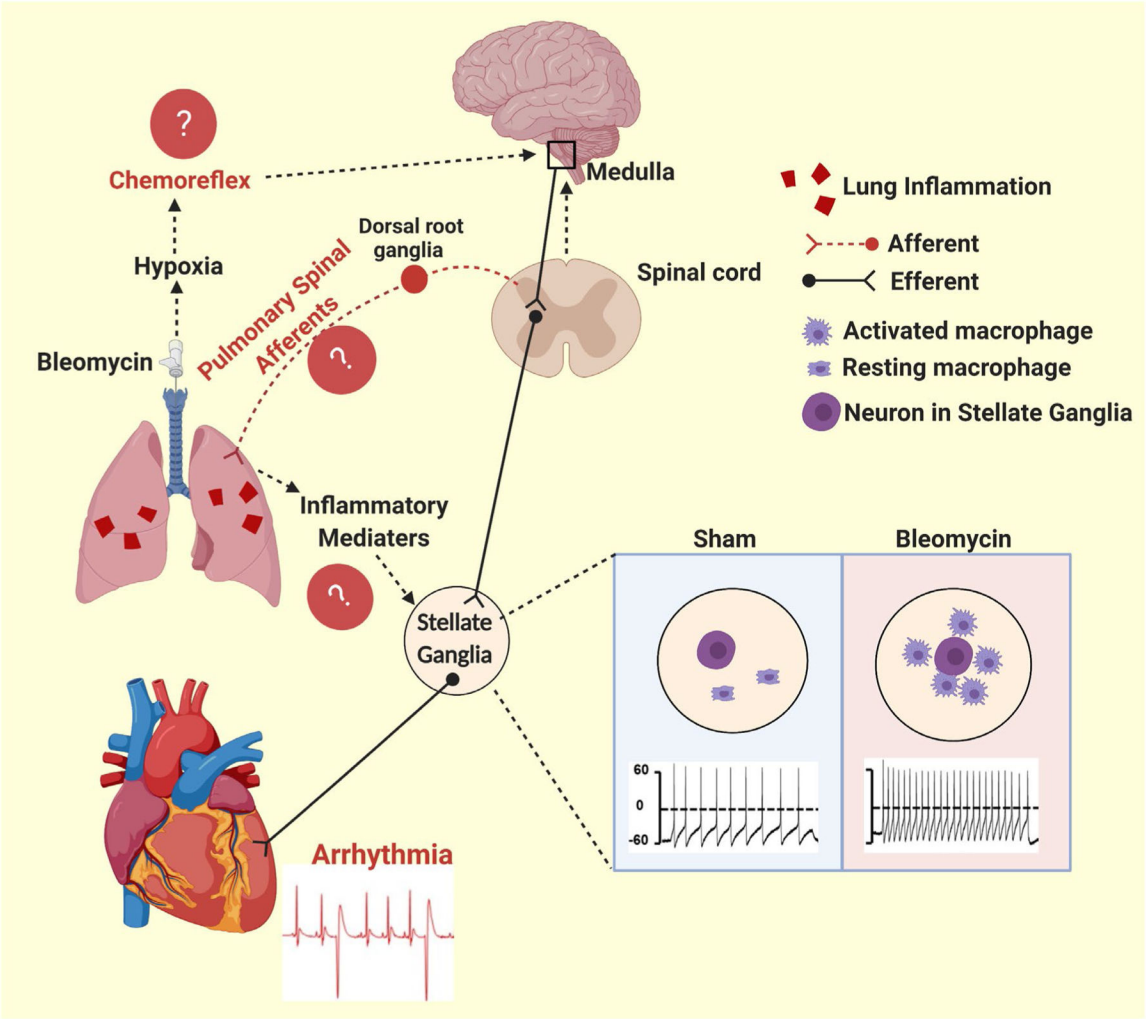

FIGURE 8.

Schematic diagram showing that macrophage activation in the SG plays a critical role in mediating acute lung injury-associated cardiac arrhythmias. Following lung injury, we observed activated macrophages in the stellate ganglia and a significant increase in cardiac premature ventricular contraction (PVC). These increased PVCs are likely caused by a complex interaction between inflammation, the lung, the heart and the central and the peripheral nervous systems. The chemoreflex and PSAR may contribute to the cardiac phenotype. The data of this study suggest that neuroinflammation of the stellate ganglia contributes directly to this cardiac phenotype